Acoustic Characteristics of a Model Isolated Tiltrotor in DNW

Earl R. Booth, Jr.
Senior Research Engineer
NASA Langley Research Center
Hampton, VA

Megan McCluer
Research Engineer
NASA Ames Research Center
Moffett Field, CA

Hormoz Tadghighi
Senior Engineering Specialist
The Boeing Company
Mesa, AZ

Abstract

An aeroacoustic wind tunnel test was conducted using a scaled isolated tiltrotor model. Acoustic data were acquired using an in-flow microphone wing traversed beneath the model to map the directivity of the near-field acoustic radiation of the rotor for a parametric variation of rotor angle-of-attack, tunnel speed, and rotor thrust. Acoustic metric data were examined to show trends of impulsive noise for the parametric variations. BVISPL maximum noise levels were found to increase with α for constant μ and C_T, although the maximum BVI levels were found at much higher α than for a typical helicopter. BVISPL levels were found to increase with μ for constant α and C_T. BVISPL was found to decrease with increasing C_T for constant α and μ, although BVISPL increased with thrust for a constant wake geometry. Metric data were also scaled for M_{tip} to evaluate how well simple power law scaling could be used to correct metric data for M_{tip} effects.

Nomenclature

c	measured speed of sound, ft/sec
C_T	thrust coefficient
f	frequency, Hz.
f_e	equivalent flat plate drag area, ft^2
M_{tip}	rotor tip Mach number, $R\Omega/c$
p/p_{norm}	non-dimensional acoustic pressure (p_{norm} is arbitrarily selected constant.)
R	rotor radius, 4.75 ft. (1.45 m)
SPL	sound pressure level, dB
V	tunnel speed, ft/sec
x/R	non-dimensional x distance, origin at hub, positive downstream
y/R	non-dimensional y distance, origin at hub, positive towards advancing side
z/R	non-dimensional z distance, origin at hub, positive up
α	rotor angle of attack, positive aft, degree
Θ_{BVI}	α for maximum BVI noise, degree
μ	advance ratio, $V/\Omega R$
ψ	rotor azimuth angle, zero when reference, blade aligned with positive x-axis, positive in the direction of rotor rotation, degree
Ω	rotor rotational velocity, radians/second

Presented at the American Helicopter Society 55th Annual Forum, Montreal, Canada, May 25-27, 1999.

Introduction

The air transportation system is becoming more congested with continued growth of the air travel industry. One method to reduce congestion at airports is to off-load some of the passenger traffic to short-haul commuter aircraft that can fly passengers from out-lying auxiliary installations to regional hub airfields, where passengers can be carried longer distances in larger aircraft. This function is currently performed by fixed-wing commuter aircraft, which, unfortunately, use the same runways as the larger passenger aircraft at the hub airports. A better solution would be to use an aircraft that did not compete with larger passenger aircraft for runway access, thus allowing for an increase in passenger throughput. A promising concept to accomplish this solution is to employ a 30 to 40 passenger commuter tiltrotor aircraft which could pick up passengers from a neighborhood vertiport and land at specially designed facilities at hub airports, thereby off-loading runway facilities. A primary obstacle to such a concept is that tiltrotor aircraft of the size required, using current technology, will likely be too noisy to be neighborhood friendly. Research is needed to reduce tiltrotor aircraft noise to make introduction of a civil tiltrotor short-haul passenger aircraft a reality.

Report Documentation Page

Form Approved
OMB No. 0704-0188

1. REPORT DATE	2. REPORT TYPE	3. DATES COVERED
MAY 1999		**00-00-1999 to 00-00-1999**

4. TITLE AND SUBTITLE	5a. CONTRACT NUMBER
Acoustic Characteristics of a Model Isolated Tiltrotor in DNW	5b. GRANT NUMBER
	5c. PROGRAM ELEMENT NUMBER
6. AUTHOR(S)	5d. PROJECT NUMBER
	5e. TASK NUMBER
	5f. WORK UNIT NUMBER
7. PERFORMING ORGANIZATION NAME(S) AND ADDRESS(ES) **NASA Ames Research Center,Moffett Field,CA,94035**	8. PERFORMING ORGANIZATION REPORT NUMBER
9. SPONSORING/MONITORING AGENCY NAME(S) AND ADDRESS(ES)	10. SPONSOR/MONITOR'S ACRONYM(S)
	11. SPONSOR/MONITOR'S REPORT NUMBER(S)

12. DISTRIBUTION/AVAILABILITY STATEMENT
Approved for public release; distribution unlimited

13. SUPPLEMENTARY NOTES

14. ABSTRACT
see report

15. SUBJECT TERMS

16. SECURITY CLASSIFICATION OF:			17. LIMITATION OF ABSTRACT	18. NUMBER OF PAGES	19a. NAME OF RESPONSIBLE PERSON
a. REPORT **unclassified**	b. ABSTRACT **unclassified**	c. THIS PAGE **unclassified**	**Same as Report (SAR)**	**10**	

Tiltrotor aircraft would obviously be expected to sound somewhat like helicopters during helicopter mode operation. However, the helicopter flight mode operation of a tiltrotor is accomplished with significantly less disk area, which requires a higher disk loading. The higher disk loading would be expected to increase loading noise. Moreover, the increase in thrust is partially accomplished by using a much higher rotor tip speed, which also strongly increases rotor noise levels. Additionally, tiltrotor blades are very thick and highly twisted when compared to typical helicopter blades, which should also have a detrimental effect on noise generation. Although it is relatively easy to predict the effects of these changes on loading and thickness noise, it is not so clear what the effect on noise sources like blade-vortex interaction (BVI) and blade-wake interaction would be, other than a qualitative assessment that they probably should be higher amplitude as well.

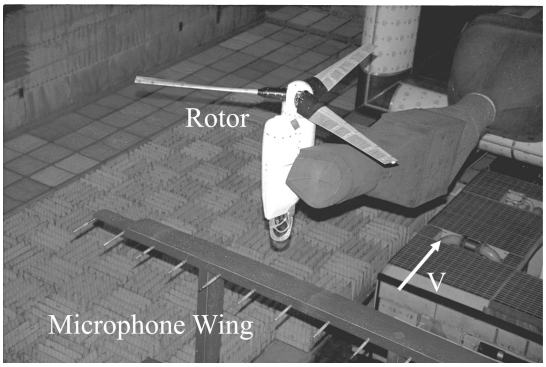

Figure 1. Isolated Rotor TRAM installed in DNW test section shown with microphone wing.

Meanwhile, a tiltrotor aircraft in airplane mode operation might be expected to sound like a turboprop aircraft. However, the diameter of a tiltrotor disk is much larger than a typical turboprop, which suggests that, with a lower than typical disk loading, a tiltrotor aircraft may be less noisy than a turboprop aircraft. Additionally, a tiltrotor aircraft propeller tip speed is usually less than the tip speed for a comparably sized turboprop aircraft, which should further reduce the noise level, so a tiltrotor aircraft has the opportunity to be quieter en-route than a comparably sized commuter turboprop aircraft.

As a result, the majority of research on tiltrotor aircraft noise has concentrated on helicopter mode operation and the current test is no exception. In fact, based on the experience of recent helicopter rotor acoustic research, it is expected that tiltrotor aircraft, like helicopters are most likely noisiest in descent conditions. Further, it is expected that BVI noise will be a dominant noise source for tiltrotor aircraft in descent conditions, as it has been for helicopters.

One way to reduce the noise of a future civil tiltrotor aircraft is to be able to predict the noise it will produce during the aircraft design phase, when major design changes are relatively inexpensive. A design tool to facilitate a design-to-noise methodology is required to enable this capability. NASA has been working, under the auspices of the Short Haul (Civil Tiltrotor) program[1] (SH(CT)) to provide such a design tool. The TiltRotor Aeroacoustic Code (TRAC)[2], however, requires a comprehensive experimental data set for validation.

A baseline aeroacoustic wind tunnel test program to obtain a comprehensive validation-quality data set including acoustic, blade surface pressure, and wake geometry data using a current-generation isolated tiltrotor model was conducted under the NASA Short Haul (Civil Tiltrotor) (SH(CT)) program using the TiltRotor Aeroacoustic Model (TRAM) in the Duits-Nederlandse Windtunnel (DNW). The test was conducted as a joint effort of NASA, U.S. Army, and Boeing. This paper will present measured acoustic results from the test. In addition, a test overview paper[3] and a paper to detail measured wake geometry data[4] will also be presented in this forum.

Test Description

The test was conducted using the isolated rotor configuration of TRAM, in the DNW, as shown in figure 1. The model consists of a quarter-scale model representing a V-22 rotor and nacelle mounted on a motor housing sting. The motor housing sting was treated with acoustic foam to reduce reflections, however, the motor housing itself blocked off a number of microphone locations on the retreating side, so definitive measurements of retreating side BVI are not possible with this model configuration. A reflection test performed with the model in the test section detected only a few measurable reflections, the largest of which were nearly 9 dB below the amplitude of the initial signal, and were ultimately shown to be reflections from the nacelle. So, reflections do not have a significant impact on the test results.

The rotor model rotor was operated at a constant rotation speed for a nominal $M_{tip} = 0.63$. Maximum rotor tip speed was defined by model drive shaft dynamic response limits, while rotor thrust was defined by power available from the motor-generator. Current technology tiltrotor aircraft tip speeds are more than ten percent greater than the tip speed used in the current wind tunnel test. This reduction in tip

speed will have several effects on the acoustic data. First, the reduction of the tip Mach number will reduce any possible noise contribution from high speed impulsive noise by a significant amount. Second, the tip speed reduction will reduce loading and thickness noise amplitudes. Further, the M_{tip} reduction will reduce the Reynolds number for each blade element which will, in turn, affect any broadband noise contributions, although by a lesser amount than the model scale. However, the primary objective of this test was to generate a data set for code validation rather than to determine absolute noise levels of a particular aircraft, so these effects were deemed to be acceptable.

Rotor angle of attack, α, was set by changing the inclination of the DNW sting, which changed the rotor shaft angle. Model geometry changes to provide shaft angle ranges appropriate for helicopter, transition, and airplane operational modes were accomplished by rotation of the nacelle and rotor about the nacelle-to-sting joint. Acoustic data were acquired for rotor operation trimmed to minimize hub gimbal angle (analogous to zero flapping in a helicopter). Data were primarily acquired for the helicopter mode configuration, with limited additional data acquired in the airplane mode configuration.

Acoustic data were acquired using a combination of in-flow traversing and out-of-flow fixed microphones. Thirteen microphones (B&K model 4134) were equally spaced from -1.86 y/R to 1.86 y/R on a traversing microphone wing (also shown in figure 1) previously used in several model helicopter acoustic tests[5,6]. In addition, two microphones (B&K model 4133) were placed outside the test section flow, one above the model and another located adjacent to the hub on the advancing side of the rotor. This paper will present data obtained with the in-flow microphones.

For each rotor test condition, the rotor hub height was maintained constant while the hub x-location was allowed to change with shaft angle. The microphone wing was traversed along a plane 1.73 z/R beneath the center of the rotor hub from -2.76 x/R to 2.76 x/R, relative to the actual rotor hub x-location for the test condition. At seventeen equally spaced locations, the traversing microphone wing motion was stopped and data were acquired. For some shaft angles, the microphone wing was not moved to the x-locations furthest downstream because of physical interference with the sting.

Acoustic data were sampled at 2048 samples per revolution, simultaneously sampling all channels, as triggered by a rotor azimuth encoder for 60 rotor revolutions. Data were then ensemble averaged in both the time and frequency domains to yield averaged time history and spectral data, respectively. The spectral data were further processed to yield OASPL, scaled-A-weighted (frequency shifted for a quarter-scale model), and band-pass BVISPL metrics (containing the acoustic energy from the 7^{th} to 50^{th} harmonic of the blade passage frequency, in the frequency band found to encompass BVI noise for this rotor) for each measurement location. Contour plots of the acoustic metrics were plotted for each microphone traverse sweep.

The test matrix was designed to provide a parametric variation of rotor angle of attack, advance ratio and thrust coefficient for code validation. Parametric trends from acoustic metric directivity contour plots, primarily the BVISPL plots, are examined in this paper. All acoustic data will be normalized in this paper, in keeping with SH(CT) programmatic requirements.

Results

Acoustic trends with α, μ, and CT will be summarized in this paper using contour plots of the acoustic metrics. The BVISPL metric plot for $\alpha = 5.0^{o}$, $\mu = 0.15$, $C_T = 0.009$ is presented in figure 2 as an example to provide contour plot formatting conventions to be used throughout the paper. The contour directivity plot represents a view from above the measurement plane, with the circle in the center representing the projection of the rotor disk onto the measurement plane. The tunnel flow direction is from the top to the bottom of the plot, which places the area upstream of the advancing side of the rotor in the upper right quarter of the plot. In this contour map, acoustic levels generated by integrating the spectral data in the frequency band specified for BVISPL at each data sampling location are contoured on a dB level basis. The dB level is represented by a color map, which is shown in the figure. All of the metric directivity data in this paper are plotted in 2 dB contour increments and use the same color map shown in figure 2.

The "x" inside the area of highest BVISPL levels represents a single microphone sampling location at x/R = -0.69, y/R = 0.93. In figures 3 and 4, the time history and spectral data from that location are plotted. Note that the time history data in figure 3 shows three strong impulsive traces for the three bladed rotor, which are typical BVI acoustic signatures. The corresponding spectral data presented in figure 4 similarly shows a typical BVI signature. Note how the frequency band of integration for BVISPL captures entirely the region in which BVI noise is dominant.

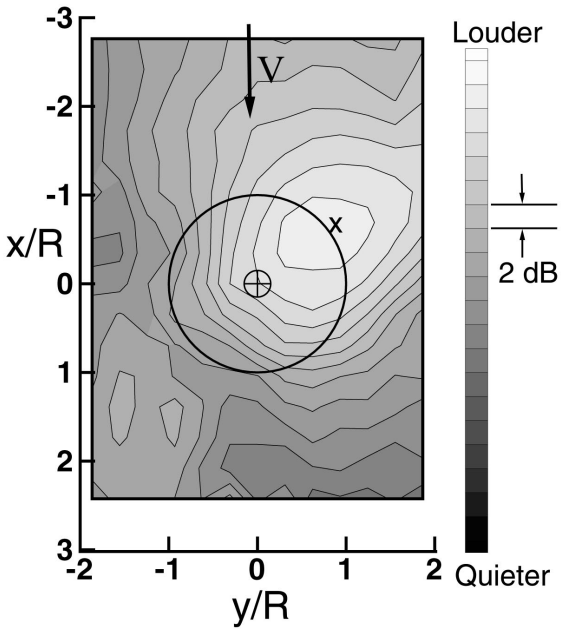

Figure 2. BVISPL contour plot for α = 0.15, μ = 5.0°, CT = 0.009.

In figure 5, metric plots for α = 0.15, μ = 5.0°, C_T = 0.009 show relative trends between metrics that hold true for the entire data set. The BVISPL metric plot shows all the energy in the band which is dominated by BVI noise and thus shows the near field directivity of BVI noise. The scaled A-weighted

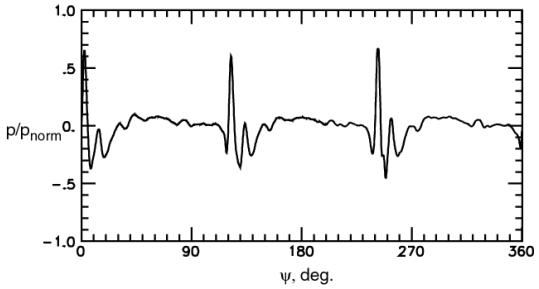

Figure 3. Time history data from x/R = -0.69, y/R = 0.93 for α = 5.0°, μ = 0.15, C_T = 0.009.

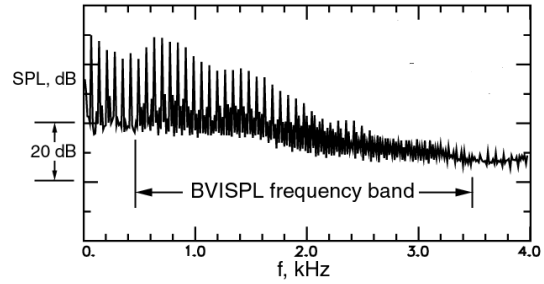

Figure 4. Spectral data from x/R = -0.69, y/R = 0.93 for α = 5.0°, μ = 0.15, C_T = 0.009.

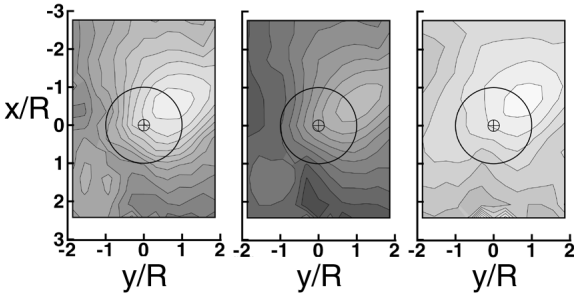

(a.) BVISPL (b.) A-Weighted (c.) OASPL

Figure 5. Metric plots for α = 5.0°, μ = 0.15, C_T = 0.009.

plot in figure 5.b. displays metric levels that are frequency scaled for a quarter-scale rotor, so that the trends displayed are applicable to a full-scale rotor. Notably, the directivity in the A-weighted plots are different from BVISPL directivity, which is due to the frequency range used in the A-weighted filtering, which does applies a significant negative weighting to a large amount of the acoustic energy present in the BVISPL frequency band. It was pointed out by Sternfeld[7], that perhaps A-weighted metrics alone did not adequately correlate with the annoyance generated by large tiltrotor aircraft, and that a combination of A-weighted and OASPL metrics was more appropriate, and the current data certainly supports that idea. In figure 5.c., the OASPL contour plot shows higher levels than even the BVISPL metric plot, which implies that low frequency loading noise is at least comparable in level to BVI noise for a large tiltrotor. This is in fact the case, as shown in figure 4. However, BVI noise tends to dominate OASPL directivity in the highest noise region making BVI noise a dominant noise source determining both amplitude and directivity of maximum noise levels. So, although the primary acoustic energy of a tiltrotor is not emphasized by the human ear, as represented by A-weighted levels, it will most likely still be annoying because of the overall sensory impact of low frequency loading, thickness, and even BVI noise. Tiltrotor noise reduction research, then, is clearly needed to make civil tiltrotor short-haul aircraft a viable option.

BVISPL noise directivity contours are shown in figure 6 for a sweep of α from 10.9° (aft tilt) to -11.0° (forward tilt). It is quite evident that the positive α cases contain much higher levels of maximum BVISPL than the negative α cases. While an positive α on the order of 10° may seem to be a bit extreme, it is representative of a level-deck descent with a glide slope on the order of 10°, which is still a bit steep, even by tiltrotor standards, but which may represent a desirable approach slope for some vertiport applications. So, BVI noise is most dominant for a

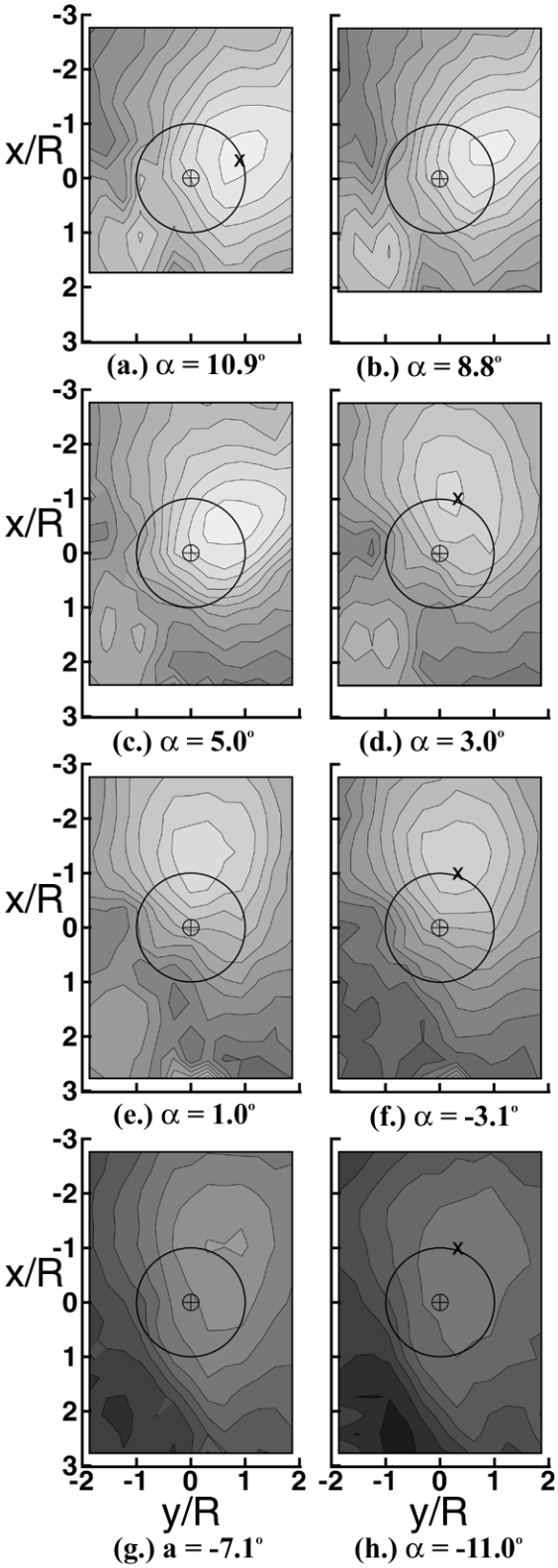

Figure 6. BVISPL directivity as a function of decreasing α for C_T = 0.009.

tiltrotor in a steep descent, which is expected based on helicopter BVI noise studies. A significant difference is that, for the tiltrotor, the α for maximum BVI noise levels are larger than for a typical helicopter. A possible explanation is that due to the higher disk loading for a tiltrotor, the vortex wake is pushed further down by the rotor, thereby increasing the blade-to-vortex miss distance, which requires a greater amount of positive α to generate enough upwash into the rotor to cause the vortex wake to interact with the rotor. In fact, figure 6 does

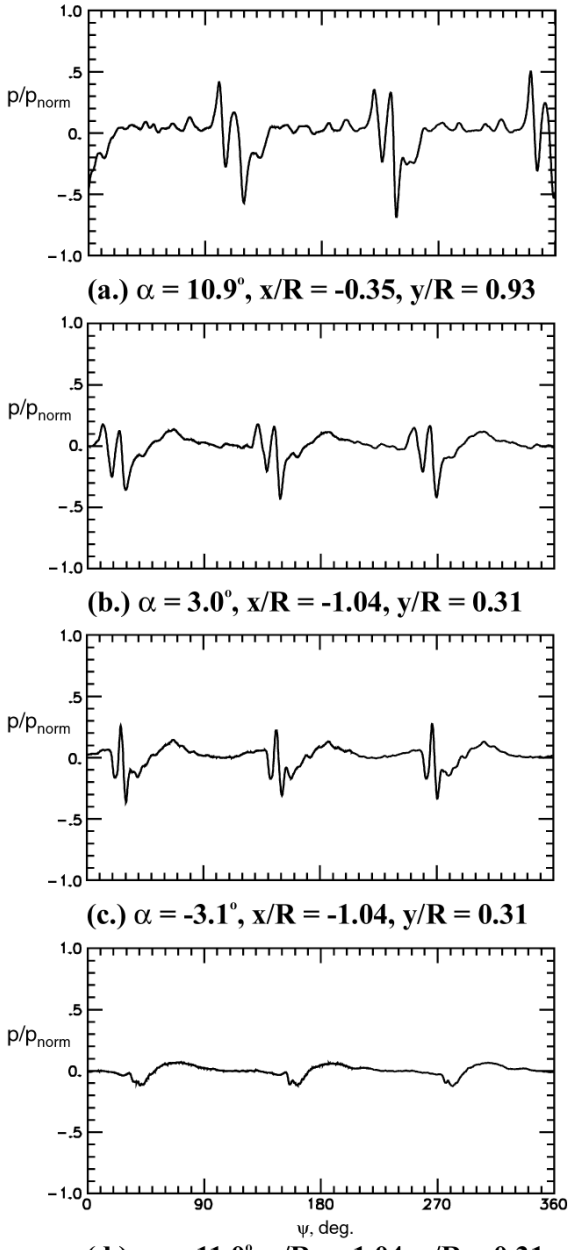

Figure 7. Time history data corresponding to conditions in figure 6.

not definitively show that the maximum BVISPL level has been reached in this α sweep, since the levels shown in figure 6.a. are the same as shown in figure 6.b., and the area enclosed by the highest BVISPL levels is actually larger in figure 6.a. In fact, there is not a great amount of difference in the BVI directivity and strength between $\alpha = 5.0^{o}$ and $\alpha = 10.9^{o}$, which is definitely not the case for a helicopter.

Interestingly, comparing figure 6.c with figure 6.d. reveals a rather abrupt change of directivity as the main BVISPL directivity lobe moves toward the front of the rotor. This change in directivity is probably due to a change in the BVI geometry. The directivity pattern remains evident from $\alpha = 3.0^{o}$ to $\alpha = -3.1^{o}$, although the levels shown in figure 6.f. are lower than shown in figure 6.d. and 6.e. In fact, the directivity pattern tends to remain even through the climb cases represented by the conditions shown in figures 6.g. and 6.h., although the maximum BVISPL levels are significantly lower for the positive α cases.

A comparison of the time history data from the locations noted by the "x" in figures 6.a., 6.d., 6.f, and 6.h. are presented in figure 7. Figure 7.a. shows an impulsive signature that indicates several strong BVI encounters. A similar signature of lesser magnitude is shown in figure 7.b., while figure 7.c. shows that one of the multiple interactions has become dominant by $\alpha = 3.1^{o}$, although the magnitude is similar to the data in figure 7.b. The time history data in figure 7.d. shows that there is very little impulsive noise present at $\alpha = -11^{o}$, which would be expected after looking at figure 6.h.

BVISPL directivity trends with decreasing α are similar for $C_T = 0.013$ at the same advance ratio, as shown in figure 8. At the higher thrust condition, the transition between forward and lateral maximum BVISPL directivity occurs more gradually between $\alpha = 8.5^{o}$, shown in figure 8.b. and $\alpha = 0.4^{o}$, in figure 8.e. The intervening cases shown in figure 8.c and 8.d., display interesting features of a transitional directivity, where multiple BVI occurrences compete for dominance. The inherent complexity of the transitional cases should provide a challenge to noise prediction codes, particularly in wake structure modeling. As was shown for the lower thrust case, the maximum BVISPL levels drop quickly with negative α.

So, BVI noise increases with α for a tiltrotor, although maximum BVI noise levels are reached at a much higher α than is the case for a helicopter. For $C_T = 0.009$, not much change in amplitude of BVI

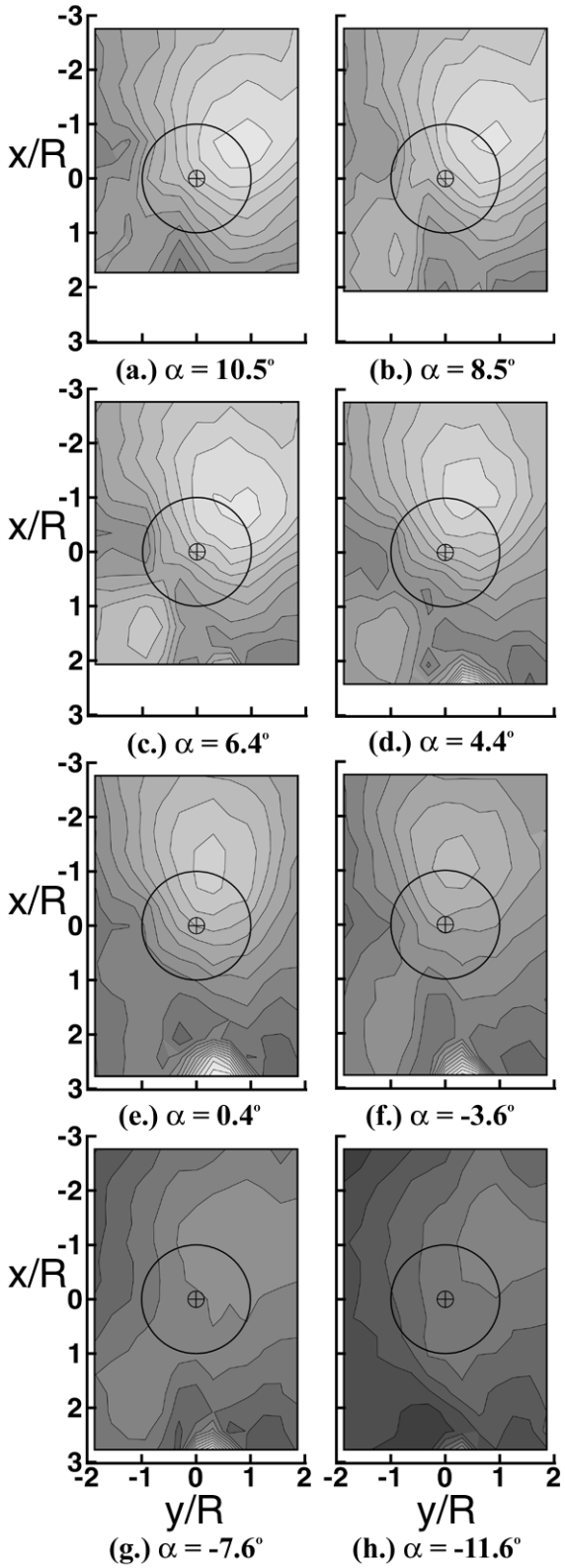

Figure 8. BVISPL directivity as a function of decreasing α for $C_T = 0.0013$

noise is experienced between $\alpha = 5.0^o$ to $\alpha = 10.9^o$, indicating a large band of descent angles that will cause a high level of BVI noise. For $C_T = 0.013$, the maximum BVISPL levels remain constant for $\alpha = 10.5^o$ to $\alpha = 4.4^o$, although directivity is not as constant in that α range as it was at the lower thrust. BVISPL levels are nearly uniform from $\alpha = 3.0^o$ to $\alpha = -3.1^o$, as well, but the levels are slightly lower than for the furthest aft α cases. Finally, for α less than -5.0^o, BVI noise is negligible.

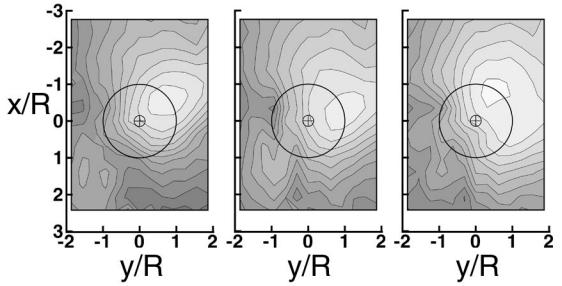

(a.) $\alpha = 5.0^o$, $\mu = 0.15$ **(b.) $\alpha = 4.2^o$, $\mu = 0.175$** **(c.) $\alpha = 5.5^o$, $\mu = 0.20$**

Figure 9. BVISPL directivity trend with increasing μ for $C_T = 0.009$.

BVI noise levels were found to increase with μ, as shown in figure 9 for $C_T = 0.009$ and α held as constant as possible using the current data set. As μ is increased from 0.15 to 0.20, not only does the maximum BVISPL level increase, but the area enclosed by the second highest contour level increases dramatically. Interestingly, the contour enclosing the highest metric level seems to change directivity, much as was shown for the α sweep in figure 6.

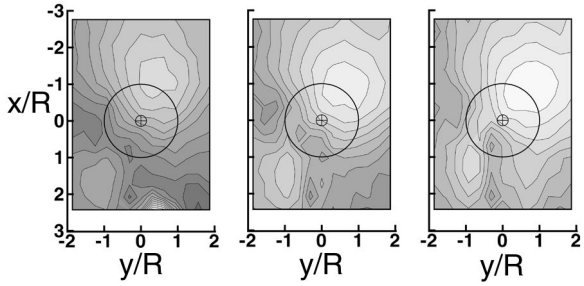

(a.) $\alpha = 4.4^o$, $\mu = 0.15$ **(b.) $\alpha = 4.9^o$, $\mu = 0.175$** **(c.) $\alpha = 5.0^o$, $\mu = 0.20$**

Figure 10. BVISPL directivity trend with increasing μ for $C_T = 0.013$.

However, the trend of BVISPL increasing with advance ratio is even more notable for $C_T = 0.013$, as shown in figure 10. As μ increases from 0.15 to 0.20, not only does the maximum BVISPL level increase, but the area encompassed by the contour enclosing the maximum level increases dramatically. In fact, it appears that even BVI levels on the retreating side increase, but due to the model sting geometry masking of some retreating side microphone locations, no definitive statements are possible. However, a general conclusion is that for α and C_T held constant, BVISPL increases with μ, at least for the limited range of μ tested.

BVISPL also displays an unexpected trend with thrust, as thrust increases, BVISPL levels decrease. In figure 10, BVISPL contour plots are presented for $C_T = 0.009$, 0.011, and 0.013 at α equal to approximately 5^o and $\mu = 0.15$. As thrust increases, the BVISPL directivity moves forward and the maximum BVISPL level decreases. This is similar to the trend shown with decreasing α in figure 6, suggesting BVISPL changes with thrust much as it changed with decreasing α. It is likely that this trend is due to an increase in the blade-to-vortex miss distance caused by a stretching of the rotor vortex wake due to increased downwash velocity for the higher thrust level cases. So the reason that the noise levels decrease is most likely due more to differences in wake geometry caused by the increased thrust rather than the effects of the increased thrust of the

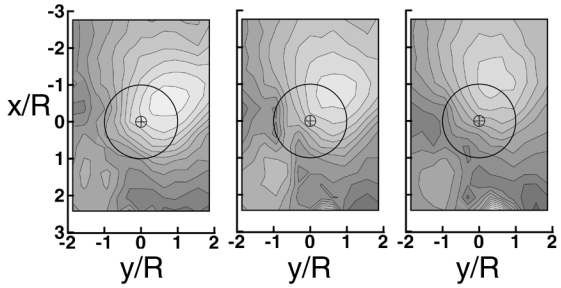

(a.) $\alpha = 5.0^o$, $C_T = 0.009$ **(b.) $\alpha = 4.8^o$, $C_T = 0.011$** **(c.) $\alpha = 4.4^o$, $C_T = 0.013$**

Figure 11. BVISPL directivity trend with increasing thrust at $\mu = 0.015$.

strength of the interaction itself. Although this suggests that BVI noise may be reduced for tiltrotor aircraft by increasing thrust-induced downwash velocity, that solution would likely not be practical for a civil tiltrotor.

A better comparison of thrust effects on the strength of BVI noise would be to compare cases where the wake geometry is equivalent, that is, where the effects of thrust on wake geometry are offset by changes in the wake due to α, resulting in a comparison where the effect of thrust on the strength of BVI noise can be sorted out from changes in BVI noise due to wake geometry changes caused by thrust. An equation was developed by Brooks[5], to determine α for which the tip path plane angle and the flow mean deflection angle are equal. It was hypothesized that this

condition would render maximum BVI noise levels since the rotor would effectively be flying in its own wake. The equation is

$$\Theta_{BVI} = \frac{90}{\pi}\left(\frac{C_T}{\mu^2}\right) + 0.44\left(\frac{\mu^2}{C_T}\right) \quad (1)$$

where Θ_{BVI} is in degrees, appropriate first order terms and small angle approximations are made for small α, and a radians-to-degrees factor is buried in the constant in the second term. The equation is valid for cases where V is much greater than the downwash velocity, which is generally true for $\mu > 0.1$, even for a highly loaded tiltrotor. Upon reexamination of the original analysis[8] and comparing it to a similar but independent analysis[9], it can be shown that the equation can be expressed as

$$\Theta_{BVI} = \frac{180}{\pi}\left(\frac{C_T}{2\mu^2} + \frac{f_e \mu^2}{2\pi R^2 C_T}\right) \quad (2)$$

where f_e is the equivalent flat plate surface area of the fuselage of the helicopter. In this case, it is more appropriate to include the extra drag caused by the wings and tail surfaces along with the fuselage. Assuming that the wake geometry for the three thrust levels are equivalent when the tip path planes are equal to the deflection angle caused by the thrust of the rotor and that the wake geometry changes with α the same for each thrust level, then equation 2 can be used to determine Θ_{BVI} for the three thrust level cases at $\mu = 0.15$ and that information can be used to select data that correspond to a constant wake geometry. Using a flat plate area appropriate for a large tiltrotor aircraft, the difference in $\alpha = \Theta_{BVI}$ between each of the thrust levels is about 2.5°.

In figure 12, the equivalent wake cases are presented and show that the maximum BVISPL level increases with thrust. Using the two-dimensional theory given by Hardin[10], the expected increase in BVI noise level due to thrust from $C_T = 0.0009$ to 0.0013 would be approximately 3.2 dB, which would represent an increase of at least one contour level, as is indeed shown in figure 12. So, although increasing thrust causes a decrease in BVISPL at constant μ and α, the effect is probably due to increases in the blade-to-vortex miss distance caused by the stretching out of the vortex wake by the high thrust loading. However, if the wake geometry is allowed to remain constant by varying α with thrust, then increasing thrust increases BVISPL, in a manner predicted by simple two-dimensional theory.

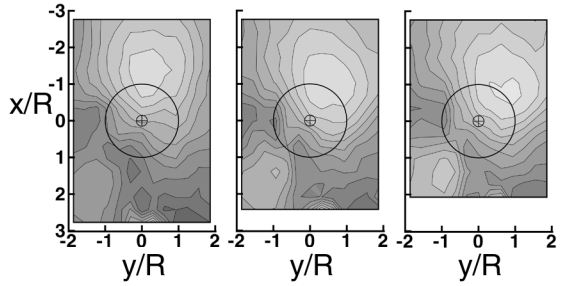

(a.) $\alpha = 1.0°$, $C_T = 0.009$ **(b.) $\alpha = 3.7°$, $C_T = 0.011$** **(c.) $\alpha = 6.4°$, $C_T = 0.013$**

Figure 12. BVISPL directivity trend with increasing thrust for constant wake geometry.

In order to investigate scaling of the data, additional data were obtained for one case of reduced M_{tip} which will be used to evaluate the applicability of simple power law scaling to the current data. The data set obtained in this test was obtained for constant rotor rotational speed rather than constant rotor tip Mach number. This was driven primarily by the data reduction requirements for extraction of broadband noise data from the acoustic data (which is not included in this paper). However, this poses a concern in that, if the speed of sound changes during the test, then the rotor tip Mach number changes along with it. Since M_{tip} is such a powerful influence on acoustic data, will the resulting change in M_{tip} change the data to a significant extent? Is it even possible to correct this effect by using first order scaling on BVISPL data? It was suggested by Leighton[11] that BVI levels follow a M_{tip}^6 power law scaling. The nominal M_{tip} for the test was 0.63. Additional data were obtained with $M_{tip} = 0.60$ at $\alpha = 5°$, $\mu = 0.15$, and $C_T = 0.009$ to explore the applicability of simple scaling on acoustic metric directivity data. The spectral data from this case were scaled in amplitude and frequency by the following equations:

$$SPL = SPL_0 + 60 \log_{10}\left(\frac{M_{tip}}{M_{tip_o}}\right) \quad (3)$$

$$f = f_o\left(\frac{M_{tip}}{M_{tip_o}}\right) \quad (4)$$

where subscript o denotes the original data.

Figure 13 compares OASPL metric directivity for $\alpha = 5°$, $\mu = 0.15$ and $C_T = 0.009$ for $M_{tip} = 0.63$ and 0.60 with scaled OASPL directivity computed from the $M_{tip} = 0.60$ data using the above equations. In this case the scaling law does a good job of recovering the directivity pattern, but not a perfect job. Since the scaling law was used to amplify all the data, rather than just data where rotor noise was dominant, it would be expected that the scaled data would not perfectly match the $M_{tip} = 0.63$ case.

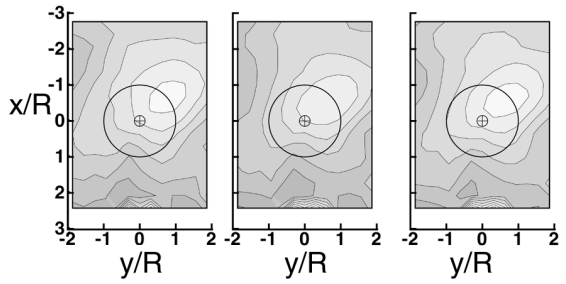

(a.) M_{tip} = 0.63 (b.) M_{tip} = 0.60 (c.) Scaled data

Figure 13. OASPL directivity scaling with M_{tip} for α = 4.9°, μ = 0.15, and C_T = 0.009.

However, the scaling would be expected to work best in the regions of highest noise levels, since the rotor noise would be most dominant in those areas. Since OASPL is an integration over the entire frequency range of the data, frequency scaling has no effect on the scaled OASPL metric plot.

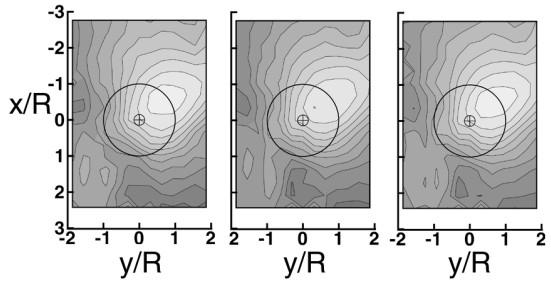

(a.) M_{tip} = 0.63 (b.) M_{tip} = 0.60 (c.) Scaled data

Figure 14. BVISPL directivity scaling with M_{tip} for α = 4.9°, μ = 0.15, and C_T = 0.009.

Similarly, since the BVISPL frequency integration range is defined in terms of blade harmonics, the acoustic energy contained in the integration should not be affected by a change in blade passage frequency, so only amplitude scaling would affect the BVISPL levels. In figure 14, the BVISPL directivity plots for the same three cases show a good recovery of the directivity with the amplitude scaling.

Although OASPL and BVISPL metrics are not affected by frequency scaling, the scaled A-weighted metric will be affected by frequency scaling. In figure 15, the scaled A-weighted metric plots are compared for the same three cases. Notice that the directivity is much better recovered than for the OASPL case. So, simple first-order scaling of spectral data for M_{tip} results in adequate scaling for OASPL levels, good scaling for BVISPL levels, and excellent scaling for A-weighted levels for a the modest M_{tip} variation used with the current data.

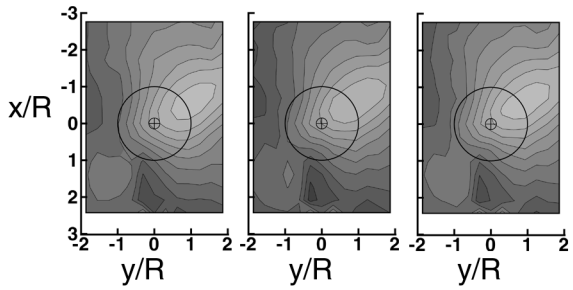

(a.) M_{tip} = 0.63 (b.) M_{tip} = 0.60 (c.) Scaled data

Figure 15. Scaled A-weighted directivity scaling with M_{tip} for α = 4.9°, μ = 0.15, and C_T = 0.009.

Conclusions

A baseline aeroacoustic data set was obtained for code validation including acoustic, blade surface pressure, and wake geometry data. The test matrix was designed to provide a parametric variation of α, μ, and C_T.

BVISPL levels were shown to increase with α and maximum BVISPL levels were found at higher shaft angles than are typical for a helicopter. A possible reason for this is the greater thrust loading for a tiltrotor which would tend to stretch out the vortex wake as compared to a typical helicopter, and thus increase blade-to-vortex miss distances, which requires a greater amount of aft tilt to generate sufficient upwash flow into the rotor to cause the vortex wake to interact with the rotor. BVI noise was shown to be negligible for α less than -5° as is consistent with previous helicopter results.

BVISPL was shown to increase with μ for α and C_T held constant, and this trend was shown to be more dramatic for the higher thrust level, both of which are expected based on helicopter noise testing. However, when α and μ are held constant and thrust is increased, maximum BVISPL levels decrease, and this was not expected. A possible explanation is that the higher thrust levels increase the blade-to-vortex miss distance by stretching out of the vortex wake geometry. However, by selecting cases with similar wake geometry, it was shown that maximum BVISPL levels increase with thrust consistent with predictions based on simple two-dimensional theory.

Finally, spectral data were scaled for tip Mach number using first order amplitude and frequency scaling laws. Metric data calculated from the scaled data showed adequate scaling of OASPL directivity, good scaling of BVISPL directivity, and excellent scaling of A-weighted directivity data.

Acknowledgments

The experimental results in this paper were derived from research performed under the auspices of the Tilt Rotor Aeroacoustic Model (TRAM) project and the NASA Short Haul Civil Tiltrotor program SH(CT). The TRAM and SH(CT) programs are led at NASA Ames Research Center by the Army/NASA Rotorcraft Division and Advanced Tiltrotor Technology Project Office, respectively. Other major funding partners and research participants in the experimental research effort were the U.S. Army Aeroflightdynamics Directorate (AFFD) located at Ames, NASA Langley Research Center Fluid Mechanics and Acoustics Division, and Boeing Information, Space, and Defense Systems (Mesa, Arizona). In addition, the outstanding support provided by the Duits-Nederlandse Windtunnel staff during the execution of the wind tunnel test was critical to the success of the test.

References

1. Marcolini, M. A., Burley, C. L., Conner, D. A., and Acree, C. W., Jr., "Overview of Noise Reduction Technology of the NASA Short Haul (Civil Tiltrotor) Program," SAE paper 962273, International Powered Lift Conference, Jupiter, FL, Nov. 8-10, 1996.

2. Burley, C. L., Marcolini, M. A., Brooks, T. F., Brand, A. C., Conner, D. A., "Tiltrotor Aeroacoustic Code (TRAC) Predictions and Comparison with Measurements", American Helicopter Society 52nd Annual Forum, Washington, D.C., June 1996.

3. Young, L. A., Booth, E. R., Yamauchi, G. K., Botha, G., Dawson, S., "Overview of the Testing of a Small-Scale Proprotor," presented at the American Helicopter Society 55th Forum, May 1999.

4. Yamauchi, G. K., Burley, C. L., Merker, E., Pengel, K., and JanakiRam, R., "Flow Measurements of an Isolated Model Tilt Rotor," presented at the American Helicopter Society 55th Forum, May 1999.

5. Brooks, T. F., Booth, E. R., Boyd, D. D., Splettstoesser, W. R., Shultz, K-J, Kube, R. , Niesl, G. H., and Streby, O., "HHC Study in the DNW to Reduce BVI Noise - an Analysis," presented at the American Helicopter Society/ Royal Aeronautical Society International Technical Specialists Meeting - Rotorcraft Acoustics and Fluid Dynamics, Philadelphia, PA, October 1991.

6. Splettstoesser, W. R., Kube, R., Seelhorst, U., Wagner, W. Boutier, A., Micheli, F., Merker, E., and Pengel, K., "Key Results from a Higher Harmonic Control Aeroacoustic Rotor Test (HART) in the German-Dutch Wind Tunnel," 21st European Rotorcraft Forum, Saint-Petersburg, Russia, August 1995.

7. Sternfeld, H., Spencer, R., and Ziegenbein, P., "Evaluation of the Impact of Noise Metrics on Tiltrotor Aircraft Design", NASA CR 198240, November 1995.

8. Brooks, T. F., Jolly, J. R., and Marcolini, M. A., "Helicopter Main-Rotor Noise - Determination of Source Contributions Using Scaled Model Data," NASA TP 2825, August 1988.

9. Boxwell, D. A., Schmitz, F. H., Splettstoesser, W. R., and Schultz, K. J., "Helicopter Model Rotor-Blade Vortex Interaction Impulsive Noise: Scalability and Parametric Variations," Journal of the American Helicopter Society, Vol. 32, No. 1, January 1987, pp 3-12.

10. Hardin, J. C., and Lamkin, S. L., "Concepts for Reduction of Blade-Vortex Interaction Noise," presented at the America Institute of Aeronautics and Astronautics Tenth Aeroacoustics Conference, Seattle, Washington, July, 1986.

11. Leighton, K. P., Hubbard, J. E., Harris, W. L., and Peele, S. E. A., "Parametric Studies and Flow Visualization of Model Helicopter Rotor Blade Slap," presented at the American Aeronautics and Astronautics Seventh Aeroacoustics Conference, Palo Alto, California, October, 1981.